Optical Beam Steering Using InGaAsP Multiple Quantum Wells

D. A. May-Arrioja, *Student Member, IEEE*, N. Bickel, and P. LiKamWa, *Senior Member, IEEE*

***Abstract*—We report an efficient optical beam steering device based on InGaAsP multiple quantum wells. An area-selective zinc in-diffusion process is used to define highly localized p-n junctions through which electrical currents are injected into the quantum wells. The extent of the lateral spreading of the electrical carriers can be optimized by selecting the appropriate diffusion depth. Using a twin-parallel-stripe structure, an optical beam at a wavelength of 1.51 μm was steered over a 17-μm range using dc electrical currents of less than 13 mA.**

***Index Terms*—Beam steering, integrated optical switch, integrated optoelectronics, optoelectronic devices.**

I. Introduction

THE RAPID expansion in optical network capacity has created a demand for increasingly versatile components. Optical beam steering devices are becoming especially important because they have a wide range of applications, such as optical memory, signal processing, laser scanning, and optical switches. A variety of methods have been used to achieve beam steering and they can be separated into free-space and integrated applications. Micromechanical (MEMS) devices are very well suited for free-space applications [1]. In fact, due to the maturity of MEMS technology, very efficient optical cross-connects based on MEMS beam steering are now commercially available [2], [3]. The majority of integrated beam steering devices that have been demonstrated employ phase-arrayed waveguides [4]–[6]. A major drawback of this method is the requirement for a large number of phase shifting elements that must be addressed individually.

Recently, a novel beam steering concept was implemented using GaAs-AlGaAs semiconductor heterostructures [7]. The device is very simple in comparison to phase-arrayed devices, but its use was limited only to pulsed applications due to the high electrical current levels required to operate the device. When a considerable amount of current is used, thermal effects degrade the performance of the device and eventually cause the device to fail. In this letter, we demonstrate the use of an area-selective zinc in-diffusion technique that significantly reduces the current consumption of the device by optimizing the spreading of the applied current. In addition, InGaAsP multiple quantum wells (MQWs) are used in the waveguide core to obtain a stronger carrier-induced index change, which also allows us to operate in the 1550-nm wavelength range. Our experimental results reveal that at 1510 nm, a 20-fold current reduction was obtained as compared to the original device, and this makes it possible to drive our device uncooled and under dc current conditions.

Manuscript received May 17, 2004; revised July 19, 2004.

The authors are with the College of Optics and Photonics, University of Central Florida, Orlando, FL 32816 USA (e-mail: dmay@mail.ucf.edu; nbickel@creol.ucf.edu; plikamwa@creol.ucf.edu).

Digital Object Identifier 10.1109/LPT.2004.839374

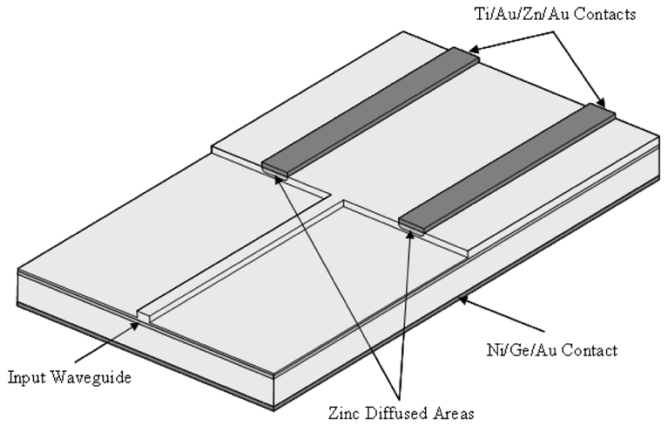

Fig. 1. Schematic drawing of integrated beam steering device.

II. Principle of Operation

A schematic drawing of the optical beam steering device is shown in Fig. 1. The input section consists of a 4-μm-wide single-mode waveguide that is 500 μm long and serves to direct the laser beam into the slab region, centered between the two contact stripes. In the slab waveguide region, two parallel contact stripes are used to inject electrical currents into the device. The stripes are each 800 μm long by 10 μm wide and are separated by a 20-μm gap. The device operates using the free carrier-induced refractive index change in semiconductors. The index of refraction of semiconductors is decreased in the presence of these free carriers through the plasma and the band-filling effects [8]. However, when MQWs are used instead of bulk semiconductors, the latter effect is significantly enhanced due to the two-dimensional density of states, such that a larger change in refractive index is observed for the same carrier density [9].

The operational principle of the device is as follows. With no current applied to the contact stripes, a laser beam that is launched into the input waveguide expands into a slab mode after propagating between the parallel electrodes. However, when electrical currents are applied through the two contact stripes, some lateral current spreading takes place in the resistive region lying between the contact and the MQW layer as a result of the finite conductivity of the semiconductor. The injected electrons accumulate in the MQW layer and spread sideways by diffusion. The density of injected electrons is highest in the MQW regions directly underneath the contacts and decreases with lateral distance. The regions that are

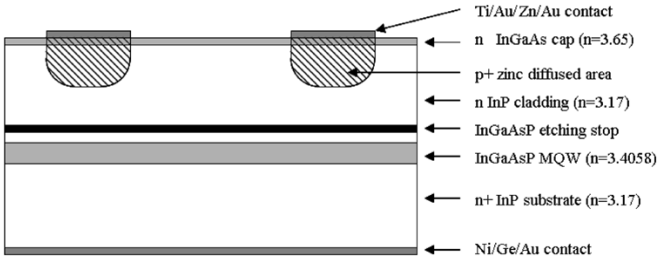

Fig. 2. Cross section of the beam steering region of the MQW planar waveguide structure showing the electrodes and the zinc diffused areas (not to scale).

saturated with electrons experience a decrease in refractive index through the carrier-induced refractive index change. Owing to the lateral distribution of the free carriers, the portion of the MQW layer between the contact stripes will form a graded-index waveguide. With equal currents, the highest refractive index is exactly centered between the contact stripes. The lateral position of the graded-index channel waveguide follows the changes in the currents injected through the stripes. When more current is applied to the right stripe than to the left stripe, the electrons underneath the right stripe spread out more, moving the induced waveguide to the left, and vice versa. By carefully controlling the ratio of the injected currents, the induced waveguide can be shifted across the entire available range, thereby steering the guided laser beam.

In the case of a regular p-i-n structure in which the whole top cladding layer is doped p-type, at very low current levels, the carriers spread out uniformly in the vicinity of the contact stripes. As the current level in each stripe is gradually increased, the finite conductivity of the p-type layer starts limiting the current spreading and causes a higher carrier density to be injected into the MQW region that is closest to the contact pads. If equal currents are injected through the two pads, the carrier density in the MQW layer between the two contacts will be lowest at the geometric center. In order for the carrier distribution to have a sufficiently sharp gradient with which to confine a waveguide mode, relatively high current injection levels (several kA/cm^2) are required [7]. Therefore, in order for the waveguiding effect to be efficient and for the device to operate with a low current density, the regions where the electrons are injected need to be set more accurately. One way of controlling the current spreading is to diffuse zinc selectively into an n-doped cladding layer, in the regions beneath the contact stripes, to obtain a low resistance current conductive window in the structure, as shown in Fig. 2. A selective-area zinc in-diffusion process [10] that enabled p-doped regions to be defined in an n-type wafer has been characterized for use in this work. By controlling the depth of the p-doped regions, the directional flow of the current can be adequately managed and the degree of current spreading can be regulated, so as to optimize the use of the injected carriers.

III. Fabrication and Experimental Results

The wafer structure used in this work is shown in Fig. 2. It was grown by metal–organic chemical vapor deposition on an n$^+$ InP substrate doped at 3×10^{18} cm^{-3}. The whole epitaxial structure was n-doped at 2×10^{17} cm^{-3} except for the MQW core region that was nominally undoped. The first layer was a 1-μm-thick InP buffer layer, followed by the MQW region that was clad by a 1.6-μm-thick InP top layer which was in turn capped by a 0.1-μm-thick InGaAs layer. The undoped MQW guiding layer consisted of 14 pairs of 100-Å-thick InGaAsP (Eg $= 0.816$ eV) quantum wells, and 100-Å-thick InGaAsP (Eg $= 1.08$ eV) barriers. A 10-nm-thick InGaAsP etch stop layer located 190 nm above the MQW was also included to allow precise control of the InP etching during the waveguide fabrication.

The device was fabricated by first depositing a 200-nm-thick silicon nitride film using plasma-enhanced chemical vapor deposition. Conventional photolithography, followed by a CF_4 plasma etching, was then used to define 10×800 μm diffusion windows in the Si_3N_4 film. The zinc in-diffusion process was performed in a semisealed open-tube diffusion furnace [10]. Zn_3P_2 was used as the zinc source to provide an over-pressure of phosphorus and to avoid degradation of the wafer surface. The sample was placed together with 100 mg of Zn_3P_2 inside a graphite box that was covered with a loose graphite lid to achieve a higher zinc vapor pressure. The depth profile of the concentration of zinc that was incorporated into the sample was measured by secondary ion mass spectroscopy (SIMS). It was found that a diffusion time of 30 min resulted in a sharp diffusion profile, with the zinc concentration slightly higher than 10^{18} cm^{-3} at the surface, and decreasing only slightly at a depth of 0.8 μm, followed by a sharp drop to the background level of the SIMS over a further 20 nm of depth. The sharp diffusion profile is consistent with other reported work [11].

After the zinc diffusion, the silicon nitride film was removed, and Ti–Au–Zn–Au p-type contacts were patterned on top of the zinc diffused areas by evaporation and liftoff. The input waveguide was then patterned by photolithography, followed by selective wet chemical etching of the InGaAs top layer with an $H_3PO_4 : H_2O_2 :$ DI water $(1 : 1 : 38)$ mixture. The InGaAs layer was then used as a mask for the selective wet chemical etching of InP with an $HCl : H_3PO_4 : CH_3CHOHCOOH$ $(2 : 5 : 1)$ mixture. The etch-stop layer provided a precise control on the etch-depth, resulting in constant height InP ridges as well as a smooth etched surface. The wafer substrate was then lapped down to a thickness of 150 μm and polished to a mirror finish. Next, the n-type contact, consisting of a mixture of Ge–Ni–Au, was deposited by thermal evaporation and annealed in. Finally, the sample was cleaved and mounted on a copper header for device testing.

The device was tested using a fiber pigtailed tunable laser. The laser beam was collimated using a fiber collimator and end-fired coupled to the input waveguide using a $40 \times$ microscope objective. The output facet was imaged using a $20 \times$ microscope objective onto a charged-coupled device camera that was connected to a television monitor. Two separate laser diode drivers were used to supply the currents to the two contact stripes. The optical beam steering device was characterized by first applying equal currents to the stripes in order to confine the laser beam to the center of the gap. Then the current in the left stripe was lowered while the current in the right stripe was increased, until the confined laser beam was pushed as far as possible from the center and to the left of the gap. By reversing these current

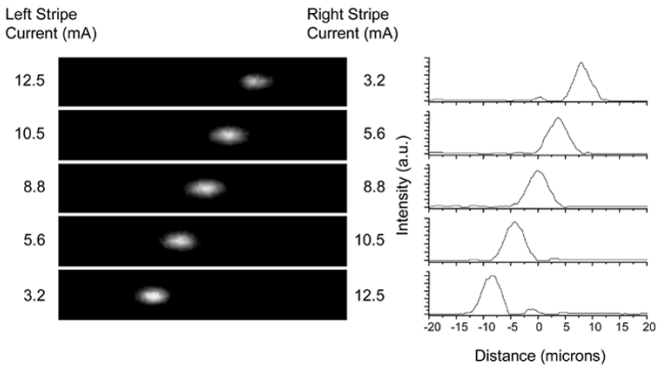

Fig. 3. Left: Images of guided beam at the output facet showing the beam being steered as the ratio of the currents is changed. Right: The corresponding near-field intensity profiles of the output beam indicating a total steering range of 17 μm.

values, the beam was then pushed to the right side of the gap. Finally, the currents were adjusted to place the beam at the intermediate positions between the center and edges of the beam steering region. The electrical currents were calibrated to obtain the highest confined mode while using the lowest possible current. It was observed that the output spot can be easily steered through most of the 20 μm spacing between the stripes. It should be noted that the intensity of the output spot did not change significantly whether it was guided to the center of device, or whether it was steered to one of the extreme positions. In a few devices that had imperfections in the metal contacts, there was a reduction of 0.8 dB when the spot was steered to the furthest off-center position.

As the laser was tuned from 1510 to 1580 nm, it was observed that the electrical current needed to perform the beam guiding and steering increased progressively, reaching 25 mA at 1580-nm wavelength. The beam steering results shown in Fig. 3 were obtained at a wavelength of 1510 nm and illustrate that, at this wavelength, the highest current needed to steer the beam to the furthest off-center position was only 12.5 mA. This represents a 20-fold reduction as compared to the previously reported work [7]. The reduction in operating current is in part due to the use of localized zinc diffusion beneath the contact stripes to control the current spreading. Additionally, the present device employs MQW in the active steering region and, therefore, a lower carrier density is needed to produce the same change in refractive index as compared to a bulk semiconductor counterpart. Ultimately, however, there is a minimum carrier density required to form a guided mode and to shift the induced waveguide to the edge of the steering region. This is what limits further current reduction given our present device configuration. The steering speed of the device has not been measured at this time. However, since the device operates by current injection, the steering speed is expected to be limited by the carrier lifetime, and therefore, nanosecond speed operation should be feasible.

IV. Conclusion

An optical beam steering device that operates with very low drive current levels has been reported. The reduction in the current levels required for beam steering is a direct consequence of effectively controlling the degree of lateral current spreading. This was achieved using an area-selective zinc in-diffusion process to form the p-n junction at an optimal diffusion depth of 0.8 μm for our steering design. Electrical current values of less than 13 mA are sufficient to achieve beam steering over a 17-μm range. With such low current values, the device was successfully operated uncooled and with dc current biases. Experiments are currently under way to achieve optical beam steering over a wider range.

References

[1] M. Kozhenikov *et al.*, "Compact 64 × 64 micromechanical optical cross connect," *IEEE Photon. Technol. Lett.*, vol. 15, no. 7, pp. 993–995, Jul. 2003.

[2] D. J. Bishop, C. R. Giles, and G. P. Austin, "The Lucent Lambdarouter: MEMS technology of the future here today," *IEEE Commun. Mag.*, vol. 40, no. 3, pp. 75–79, Mar. 2002.

[3] P. B. Chu, S.-S. Lee, and S. Park, "MEMS: The path to large optical crossconnects," *IEEE Commun. Mag.*, vol. 40, no. 3, pp. 80–87, Mar. 2002.

[4] T. Pertsch, T. Zentgraf, U. Peschel, A. Bräuer, and F. Lederer, "Beam steering in waveguide arrays," *Appl. Phys. Lett.*, vol. 80, no. 18, pp. 3247–3249, May 2002.

[5] Q. W. Song, X.-M. Wang, R. Bussjager, and J. Osman, "Electro-optic beam-steering device based on a lanthanum-modified lead zirconate titanate ceramic wafer," *Appl. Opt.*, vol. 35, no. 17, pp. 3155–3162, Jun. 1996.

[6] F. Vasey, F. K. Reinhart, R. Houdré, and J. M. Stauffer, "Spatial optical beam steering with an algaas integrated phased array," *Appl. Opt.*, vol. 32, no. 18, pp. 3220–3232, Jun. 1993.

[7] X. Dong, P. LiKamWa, J. Loehr, and R. Kaspi, "Current-induced guiding and beam steering in active semiconductor planar waveguide," *IEEE Photon. Technol. Lett.*, vol. 11, no. 7, pp. 809–811, Jul. 1999.

[8] B. R. Bennett, R. A. Soref, and J. A. del Alamo, "Carrier-induced change in refractive index of InP, GaAs, and InGaAsP," *IEEE J. Quantum Electron.*, vol. 26, no. 1, pp. 113–122, Jan. 1990.

[9] J.-I. Shim, M. Yamaguchi, P. Delansay, and M. Kitamura, "Refractive index and loss changes produced by current injection in InGaAs(P)-InGaAsP multiple quantum-well waveguides," *IEEE J. Sel. Topics Quantum Electron.*, vol. 1, no. 2, pp. 408–415, Jun. 1995.

[10] T. H. Weng, "A comparative study of p-type diffusion in III–V compound semiconductors," in *Proc. Electron Devices Meeting*, Hong Kong, Hong Kong, 1997, pp. 120–122.

[11] I. Yun and K.-S. Hyun, "Zinc diffusion process investigation if InP-based test structures for high-speed avalanche photodiode fabrication," *Microelectron. J.*, vol. 31, no. 8, pp. 635–639, Aug. 2000.